Received: 13 October 2022 | Revised: 24 April 2023 | Accepted: 7 May 2023

https://doi.org/10.1016/j.jtha.2023.05.008

ORIGINAL ARTICLE

Platelet zinc status regulates prostaglandin-induced signaling, altering thrombus formation

Charlie A. Coupland[1] | Leigh Naylor-Adamson[1] | Zoe Booth[1] | Thomas W. Price[2] | Helio M. Gil[2] | George Firth[2] | Michelle Avery[1] | Yusra Ahmed[1] | Graeme J. Stasiuk[2] | Simon D. J. Calaminus[1]

[1]Centre for Biomedicine, Hull York Medical School, University of Hull, Hull, UK

[2]Department of Imaging Chemistry and Biology, School of Biomedical Engineering and Imaging Sciences, King's College London, London, UK

Correspondence
Simon Calaminus, Centre for Biomedicine, Hull York Medical School, University of Hull, Wolfson Building, Cottingham Road, University of Hull, Hull, HU6 7RX, UK.
Email: simon.calaminus@hyms.ac.uk

Funding information
British Heart Foundation; PhD studentships Grant Number: FS/19/38/34441 (to C.A.C.) and FS/16/62/32220 (to M.A.) University of Hull (PhD fellowships [to Z.B. and Y.A.]) MRC; Grant Number: MR/T002573/1 (to G.J.S., T.W.P., and L.N.-A.).

Abstract

Background: Approximately 17.3% of the global population exhibits an element of zinc (Zn^{2+}) deficiency. One symptom of Zn^{2+} deficiency is increased bleeding through impaired hemostasis. Platelets are crucial to hemostasis and are inhibited by endothelial-derived prostacyclin (prostaglandin I_2 [PGI_2]), which signals via adenylyl cyclase (AC) and cyclic adenosine monophosphate signaling. In other cell types, Zn^{2+} modulates cyclic adenosine monophosphate concentrations by changing AC and/or phosphodiesterase activity.

Objectives: To investigate if Zn^{2+} can modulate platelet PGI_2 signaling.

Methods: Platelet aggregation, spreading, and western blotting assays with Zn^{2+} chelators and cyclic nucleotide elevating agents were performed in washed platelets and platelet-rich plasma conditions. *In vitro* thrombus formation with various Zn^{2+} chelators and PGI_2 was assessed in whole blood.

Results: Incubation of whole blood or washed platelets with Zn^{2+} chelators caused either embolization of preformed thrombi or reversal of platelet spreading, respectively. To understand this effect, we analyzed resting platelets and identified that incubation with Zn^{2+} chelators elevated $pVASP^{ser157}$, a marker of PGI_2 signaling. In agreement that Zn^{2+} affects PGI_2 signaling, addition of the AC inhibitor SQ22536 blocked Zn^{2+} chelation–induced platelet spreading reversal, while addition of Zn^{2+} blocked PGI_2-mediated platelet reversal. Moreover, Zn^{2+} specifically blocked forskolin-mediated AC reversal of platelet spreading. Finally, PGI_2 inhibition of platelet aggregation and *in vitro* thrombus formation was potentiated in the presence of low doses of Zn^{2+} chelators, increasing its effectiveness in inducing platelet inhibition.

Manuscript handled by: Katsue Suzuki-Inoue

Final decision: Katsue Suzuki-Inoue, 8 May 2023

Conclusion: Zn^{2+} chelation potentiates platelet PGI_2 signaling, elevating PGI_2's ability to prevent effective platelet activation, aggregation, and thrombus formation.

KEYWORDS
adenylyl cyclase, bleeding, prostacyclin, zinc (Zn^{2+})

1 | INTRODUCTION

Approximately 17.3% of the global population has inadequate Zn^{2+} intake either through a lack of dietary Zn^{2+} or impaired absorption [1]. Zn^{2+} is an essential bioactive trace element, which acts as a cofactor that catalyzes the reactions of approximately 10% of all enzymes in the human body [2]. As such, Zn^{2+} deficiency causes multiple physiologic effects, including stunted growth, hypogonadism, impaired wound healing, immune dysfunction, and bleeding [3–5]. The role of Zn^{2+} in hemostasis is thought to be, in part, due to its function in platelet activation [6].

Platelets are small (2-3 μm), anucleate blood cells with an average lifespan of 8 to 10 days in humans [7–9]. They are an essential component of hemostasis as they prevent blood loss at the site of injury by forming a platelet plug. Upon vascular insult, platelets are activated by exposed extracellular matrix proteins, such as collagen, von Willebrand factor, and soluble agonists such as thrombin. These compounds bind to specific receptors on the platelet outer membrane, which activates multiple intracellular signaling cascades, causing secretion of platelet alpha and dense granules. Granule secretion releases an abundance of platelet agonists such as adenosine diphosphate (ADP), serotonin, thrombospondin-1, and ions such as Mg^{2+}, Ca^{2+}, and, importantly, Zn^{2+} [10–12]. These agonistic molecules then either bind to platelet surface receptors or re-enter the platelet cytosol to proliferate platelet activation and promote thrombus formation.

Zn^{2+}, a metal ion stored and secreted by platelets, has been demonstrated to be a powerful platelet agonist (at concentrations of 0.3-1 mM) [13]. Moreover, Zn^{2+} stimulation has been demonstrated to create a flux in reactive oxygen species in platelets [14], while recent studies have shown that exogenous Zn^{2+} can enter platelets and function as an intracellular second messenger [15]. Conversely, rats fed a low-Zn^{2+} diet had decreased reactivity to ADP and impaired Ca^{2+} mobilization from the smooth endoplasmic reticulum and extracellular sources [16], while removal of Zn^{2+} from human platelets with the Zn^{2+} chelator *N,N,N',N'*-tetrakis(2-pyridylmethyl)ethylenediamine (TPEN) inhibited thrombin-induced platelet activation, platelet aggregation, and platelet spreading [15]. However, as the plasma concentration of Zn^{2+} is only estimated to be between 10 and 20 μM, importantly, it has been shown that small increases in plasma Zn^{2+} concentration have been observed to potentiate platelet aggregation [17,18].

In other cell types, Zn^{2+} plays an additional key role in the control of cyclic adenosine monophosphate (cAMP) signaling [19,20]. In platelets, cAMP is elevated by compounds, such as prostaglandin I_2 (PGI_2), that increase adenylyl cyclase (AC) activity. This elevation of cAMP induces protein kinase A (PKA) activity. This, alongside nitric oxide signaling, works to globally inhibit platelet function [21] through phosphorylation of multiple proteins [22], including the commonly used marker $VASP^{ser157}$. Phosphorylation of vasodilator-stimulated phosphoprotein (VASP) by PKA has been shown to reduce platelet activity through inhibition of VASP-mediated actin nucleation and consequent stress fiber formation [23] as well as reduction in integrin $\alpha_{IIb}\beta_3$ activity [24]. Crucially, platelet inhibition is overwhelmed at the site of vascular injury via ADP-mediated AC inhibition and activation of phosphodiesterase (PDE) [25,26].

The role of Zn^{2+} in PGI_2 signaling is currently poorly unexplored in platelet biology. Katsel et al. [27] cloned platelet AC III into HEK293 cells and demonstrated that incubation with Zn^{2+} could inhibit the enzyme in a dose-dependent manner, reducing cAMP production. This concurs with a study by Klein et al. [20], who demonstrated that incubation with low micromolar doses of Zn^{2+} could inhibit cAMP production in neuroblastoma cells. However, no further work has been conducted to our knowledge in this area. Therefore, we aimed to investigate the role Zn^{2+} plays in platelet PKA signaling and to identify if Zn^{2+} plays a key potential role in the regulation of platelet inhibition. Here, our findings demonstrate that Zn^{2+} can directly regulate PGI_2 platelet inhibition, most likely through regulation of AC activity. Zn^{2+} chelation, therefore, leads to stimulation of basal AC activity, which can also in turn potentiate PGI_2 inhibition of platelet activation. This may explain why Zn^{2+}-deficient patients have a bleeding diathesis.

Essentials

- Zinc (Zn^{2+}) deficiency causes a bleeding diathesis, and the mechanisms behind this remain unclear.
- Zn^{2+} inhibits cyclic adenosine monophosphate (cAMP) signaling, a key platelet inhibitory signaling cascade, in other cell types.
- We found that cationic Zn^{2+} can inhibit platelet prostaglandin I_2 (PGI_2)-cAMP-protein kinase A signaling.
- Zn^{2+} chelation potentiates PGI_2 activity, underpinning why Zn^{2+} deficiency can induce bleeding.

2 | METHODS

2.1 | Materials

PGI_2 and prostaglandin E_2 (PGE_2) were purchased from Cayman Chemical. Collagen Reagens HORM Suspension was purchased from Takeda, and fibrinogen was purchased from Enzyme Research. TPEN, SQ22536, and milrinone were purchased obtained from Tocris. 2-((2-(2-(2-aminoethoxy)ethoxy)ethyl)amino)-N-(quinolin-8-yl)acetamide (AQA-NOON) and 2-((2-(2-fluoroethoxy)ethyl)amino)-N-(quinolin-8-yl)acetamide (AQA-F) were synthesized according to methods described below. ProLong Diamond Antifade Mountant and paraformaldehyde (PFA) were purchased from ThermoFisher Scientific. $pVASP^{ser157}$ and pPKA substrate (RRXS*/T*) (100G7E) antibodies were obtained from Cell Signalling Technology. 3,3'-dihexyloxacarbocyanine iodide, fluorescein isothiocyanate-phalloidin, and D-Phe-Pro-Arg-chloromethylketone were purchased from Enzo Life Sciences. Vena8 Endothelial+ Microfluidic Biochip was purchased from Celix. Fluorescent secondary anti-mouse 800 and anti-rabbit 680 antibodies were purchased from LI-COR Biotechnology. Forskolin was obtained from Sigma-Aldrich. All other chemicals were obtained from Sigma Ltd unless otherwise stated.

2.2 | Platelet preparation

For platelet-rich plasma (PRP), whole blood was collected into trisodium citrate (0.109 M) using a 1:10 dilution and then centrifuged at 700 rpm for 10 minutes. Plasma was removed, and the blood was respun at 900 rpm for 10 minutes. The plasma was removed again and added to the previous PRP. For washed platelets, whole blood was collected into acid citrate dextrose (113.8 mM D-glucose anhydrase, 29.9 mM trisodium citrate, 72.6 mM sodium chloride, and 2.9 mM citric acid [pH: 6.4]) and platelets were isolated as previously described [28] without supplementation with apyrase, indomethacin, or ethylene glycol tetraacetic acid (EGTA).

2.3 | Platelet spreading

Fibrinogen (100 μg/mL)-coated coverslips were prepared as per a study by Yusuf et al. [29]. Washed platelets (2×10^7/mL) were pretreated with Tyrode, SQ22536 (100 μM), zinc sulfate ($ZnSO_4$; Zn^{2+}, 100 μM), TPEN (30 μM), AQA-F (100 μM), or AQA-NOON (1 mM) and then spread for 25 minutes. Platelets were then washed and post-treated with Tyrode, TPEN (30 μM), AQA-F (100 μM), AQA-NOON (1 mM), SQ22536 (100 μM), 1,2-Bis(2-aminophenoxy)ethane-N,N,N′,N′-tetraacetic acid tetrakis(acetoxymethyl ester) (BAPTA-AM [30 μM]), PGI_2 (10 nM), PGE_2 (100 nM), milrinone (10 μM), or forskolin (10 μM) for 20 minutes. After treatment, platelets were fixed in 4% PFA for 10 minutes before permeabilization in 0.1% Triton X-100 for 5 minutes and mounting with ProLong Diamond Antifade Mountant. Slides were stained with fluorescein isothiocyanate-phalloidin for 30 minutes at room temperature, washed in phosphate-buffered saline, and imaged on a Zeiss Axio Imager fluorescence microscope with a ×63 oil immersion objective (1.4 NA) using Zen Pro software (Zeiss). Five images were taken per condition. Platelet adhesion, platelet surface area, and number of platelets with actin nodules or stress fibers were analyzed using ImageJ (National Institutes of Health). Platelets were identified as containing nodules if they had at least 2 nodules present. If it was not possible to identify any actin structures within the platelets, these were classed as unclassifiable.

2.4 | Platelet aggregation

For studies with Zn^{2+} chelators, washed platelets (2.5×10^8/mL) or PRP were stirred at 1200 rpm at 37 °C and incubated for up to 18 minutes with AQA-NOON (100 μM-1 mM), TPEN (3-50 μM), or AQA-F (10-100 μM). Dependents on the experiment samples were then treated with Tyrode, $ZnSO_4$ (Zn^{2+}, 50 μM), PGE_2 (10 nM), or PGI_2 (5 nM) for 2 minutes before stimulation with collagen (10 μg/mL), $ZnSO_4$ (Zn^{2+}, 300 μM), or thrombin (0.1 U/mL) for up to 5 minutes.

For Zn^{2+} aggregation experiments, washed platelets (2.5×10^8/mL) were incubated under stirring conditions for 2 minutes prior to stimulation with Tyrode or $ZnSO_4$ (Zn^{2+}, 10 μM-1 mM).

For all experiments, platelet aggregation was monitored for up to 5 minutes using a CHRONOLOG Model 490 aggregometer using AGGRO/LINK Opti8 software (Chronolog).

2.5 | *In vitro* thrombus formation under flow

Microfluidic biochips were coated with collagen (25-100 μg/mL) overnight and then blocked with denatured bovine serum albumin (5 mg/mL) for 15 minutes. Whole blood was treated with D-Phe-Pro-Arg-chloromethylketone (20 μM) and stained with 3,3'-dihexyloxacarbocyanine iodide (10 μM) prior to flow for all experiments. For thrombus formation experiments, chelators (AQA-NOON [300 μM], AQA-F [10 μM], or TPEN [3 μM]) were incubated with whole blood for 20 minutes, followed by addition of PGI_2 (300 pM) for 2 minutes. Whole blood was then flowed over collagen (25 μg/mL) at 1000 s^{-1} for 2 minutes, washed with phosphate-buffered saline, and fixed with 4% PFA. For thrombus stability experiments, whole blood was flowed over collagen (100 μg/mL) at 1000 s^{-1} for 4 minutes, followed by postflow with Tyrode supplemented with or without chelators (AQA-NOON [1 mM], AQA-F [100 μM], or TPEN [30 μM]) for 10 minutes. After treatment, thrombi were fixed with 4% PFA. For all experiments, thrombi were imaged using a Apotome.2 confocal unit on Zeiss Axio Observer with a ×63 oil immersion objective (1.4 NA) and Zen Pro software. Five images were taken per condition. Total thrombus surface area coverage was analyzed using ImageJ. Thrombus height was analyzed using ZEN 3.5 (Blue edition, Zeiss).

2.6 | Immunoblotting

Washed platelets (4×10^8/mL) were treated with AQA-NOON (1 mM), AQA-F (100 μM), TPEN (30 μM), or Tyrode for 20, 30, and 40 minutes before lysis with Laemmli buffer. PGI_2 (5 nM) was incubated with washed platelets, and samples were taken at 2, 10, and 20 minutes and lysed with Laemmli buffer. Samples were fractionated by sodium dodecyl sulfate-polyacrylamide gel electrophoresis before transfer to nitrocellulose; western blotted with specific primary antibodies for $pVASP^{ser157}$, GAPDH, or pPKA substrate; and visualized using Licor Odyssey CLx (LI-COR Laboratories). Densitometry was measured via Image Studio (version 5.2, LI-COR Laboratories). Fold change ($pVASP^{ser157}$/GAPDH) was normalized to the control.

2.7 | AQA-NOON synthesis

All chemicals were purchased from Sigma-Aldrich and used without purification. 2-chloro-N-(quinoline-8-yl)acetamide was prepared according to previously published methods [30].

To the prepared 2-chloro-N-(quinolin-8-yl)acetamide (4.85 g, 22 mmol, 1 eq), 2,2'-(ethylenedioxy)bis(ethylamine) (17 mL, 17.26 g, 116 mmol, 5.3 eq), potassium iodide (258 mg, 1.55 mmol, 0.07 eq), and N,N-diisopropylethylamine (13.6 mL, 10.09 g, 78 mmol, 3.5 eq) were added. The solution was heated to 90 °C overnight.

After cooling to room temperature, the solution was poured into water (200 mL) and extracted with dichloromethane (3 × 200 mL). The combined organic layers were dried with magnesium sulfate, filtered, and concentrated to afford a dark-red oil (5.58 g, 16.7 mmol, 76%).

2.8 | AQA-NOON characterization data

To characterize the dark-red oil produced at the end of synthesis, Nuclear Magnetic Resonance (NMR) measurements were performed on a Bruker Avance III HD NanoBay 400 MHz NMR spectrometer. Chemical shifts (δ) were reported in parts per million referenced to the residual solvent peak. Multiplicities of observed peaks are denoted by s (singlet), d (doublet), t (triplet), q (quartet), quin (quintet), m (multiplet), and br (broad). Coupling constants of signals are reported as *J* values with the unit of Hertz. See NMR characterization data below.

^{1}H NMR [$CDCl_3$, 400 MHz, 298 K], δ: 11.36 (br s, 1 H), 8.85 (dd, 1 H, $^3J_{HH}$ = 4.2 Hz, $^4J_{HH}$ = 1.7 Hz), 8.81 (dd, 1 H, $^3J_{HH}$ = 7.1 Hz, $^4J_{HH}$ = 1.9 Hz), 8.15 (dd, 1 H, $^3J_{HH}$ = 8.3 Hz, $^4J_{HH}$ = 1.7 Hz), 7.54 (dd, 1 H, $^3J_{HH}$ = 8.3, 7.1 Hz), 7.51 (dd, 1 H, $^3J_{HH}$ = 8.3 Hz, $^4J_{HH}$ = 1.9 Hz), 7.45 (dd, 1 H, $^3J_{HH}$ = 8.3, 4.2 Hz), 3.73 (t, 2 H, $^3J_{HH}$ = 5.1 Hz), 3.68-3.61 (m, 4 H), 3.57 (s, 2 H), 3.52 (t, 2 H, $^3J_{HH}$ = 5.2), 2.94 (t, 2H, $^3J_{HH}$ = 5.1), 2.87 (t, 2 H, $^3J_{HH}$ = 5.2 Hz).

^{13}C NMR [$CDCl_3$, 100 MHz, 298 K], δ: 170.84, 148.62, 139.17, 136.36, 134.49, 128.23, 127.48, 121.83, 121.65, 116.74, 73.80, 70.83, 70.55, 70.41, 53.77, 49.53, 41.82.

2.9 | Metal binding titrations

Metal chloride in 4-(2-hydroxyethyl)-1-piperazineethanesulfonic acid solution (10 mM; pH, 7.4) was added to a solution of AQA-NOON (100 μM) in 4-(2-hydroxyethyl)-1-piperazineethanesulfonic acid (10 mM; pH, 7.4). Spectra were recorded on a Perkin-Elmer Lambda 365 spectrofluorometer. Data were analyzed using GraphPad Prism 9.0.0 (GraphPad) and fitted using a 1-phase association.

2.10 | AQA-F synthesis

For AQA-F synthesis, refer to the study by Price et al. [30].

2.11 | TPEN and AQA-F metal binding affinity

For metal binding affinity calculation methods for AQA-F, refer to the study by Price et al. [30], and for TPEN, refer to the study by Shumaker et al. [31].

2.12 | Donor recruitment

Written informed consent was acquired for donation of blood. Blood was obtained from healthy drug-free volunteers in accordance with relevant health and safety guidelines under ethical permission granted by the Hull York Medical School Ethics Committee for "The study of platelet activation, signalling and metabolism" and the National Health Service (NHS) Research Ethics Committee (REC) study "Investigation of blood cells for research into cardiovascular disease" (21/SC/0215).

2.13 | Statistical analysis

Data are presented as mean ± SEM. Data were arcsine transformed as appropriate prior to statistical analysis to transform percentage data to numerical data to meet the requirements for performing paired *t*-test or 1-way analysis of variance. Statistical analysis was performed using either paired *t*-test or repeated-measure 1-way analysis of variance. In case normality was not met, significance was calculated using the nonparametric Kruskal-Wallis test (GraphPad Prism 8.0.1 software). Significance is defined as $p < .05$.

3 | RESULTS

3.1 | Zn^{2+} is required to maintain platelet spreading and thrombus stability

Zn^{2+} is a direct platelet agonist, stimulating platelet aggregation in a dose-dependent manner (Supplementary Figure S1), while Zn^{2+} chelation inhibits platelet aggregation [13]. To further understand the role

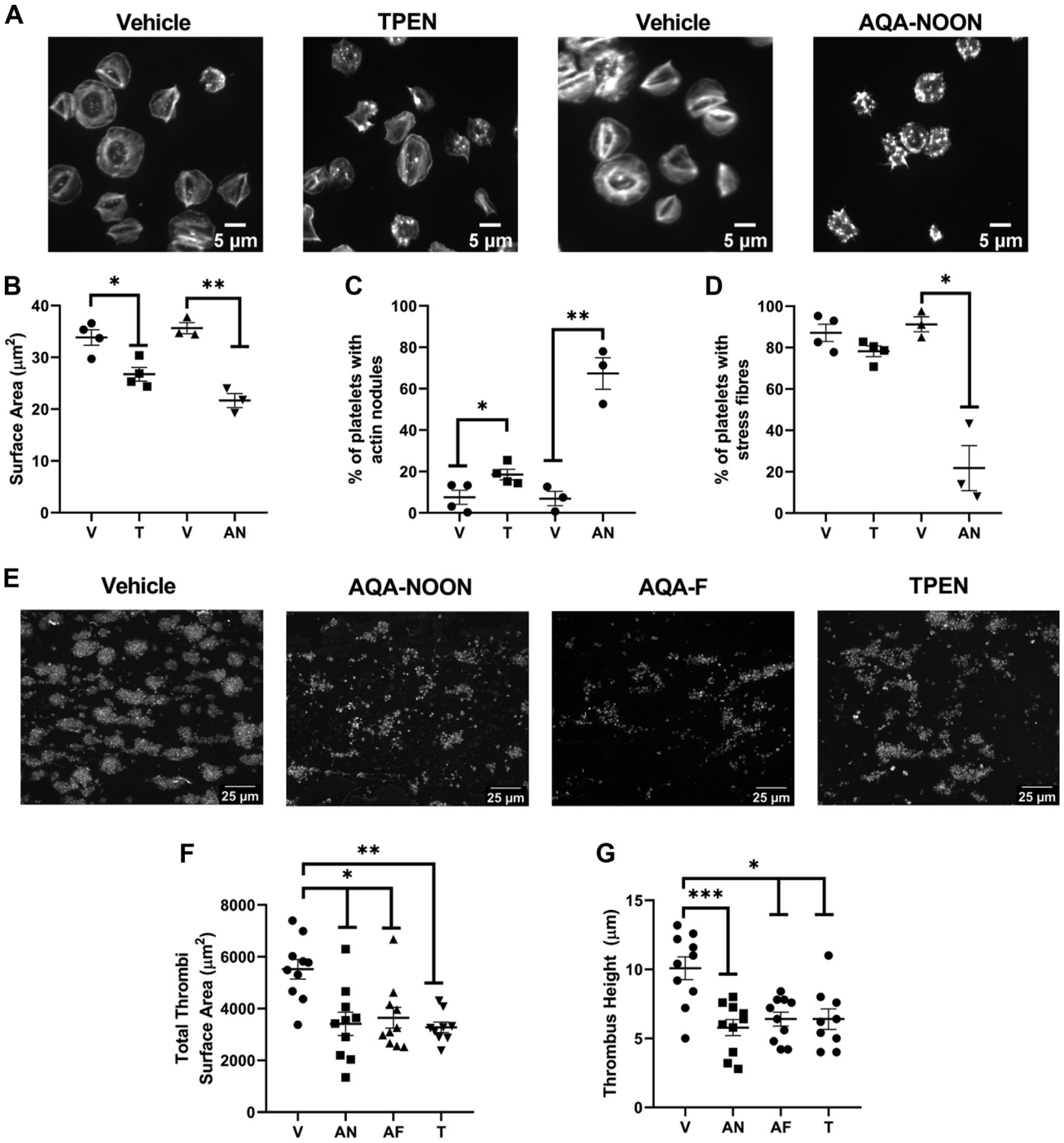

FIGURE 1 Zinc is required for maintenance of platelet activity and thrombus formation. For spreading, platelets (2×10^7/mL) were spread on fibrinogen (100 µg/mL) for 25 minutes. They were then washed with phosphate-buffered saline and treated with Tyrode (vehicle), *N*,*N*,*N*',*N*'-tetrakis(2-pyridylmethyl)ethylenediamine (TPEN; 30 µM), or 2-((2-(2-(2-aminoethoxy)ethoxy)ethyl)amino)-N-(quinolin-8-yl)acetamide (AQA-NOON; 1 mM) for 20 minutes. For *in vitro* thrombus formation, preformed thrombi were treated with Tyrode (vehicle), AQA-NOON (1 mM), 2-((2-(2-fluoroethoxy)ethyl)amino)-N-(quinolin-8-yl)acetamide (AQA-F; 100 µM), or TPEN (30 µM) for 10 minutes. (A) Representative images. Scale bar is 5 µm. (B) Average surface area of spread platelets. (C) Percentage of platelets with actin nodules. (D) Percentage of platelets with stress fibers. (E) Representative images of *in vitro* thrombus formation. (F) Total surface area covered by thrombi (µm²). (G) Thrombus height (µm). Spreading data: n = 4 (TPEN) and n = 3 (AQA-NOON). *In vitro* thrombus formation data: n = 9 (TPEN) and n = 10 (AQA-NOON, AQA-F). Data are presented as mean ± SEM. *$p < .05$, **$p < .01$, and ***$p < .001$. AF, AQA-F; AN, AQA-NOON; T, *N*,*N*,*N*',*N*'-tetrakis(2-pyridylmethyl) ethylenediamine; V, vehicle.

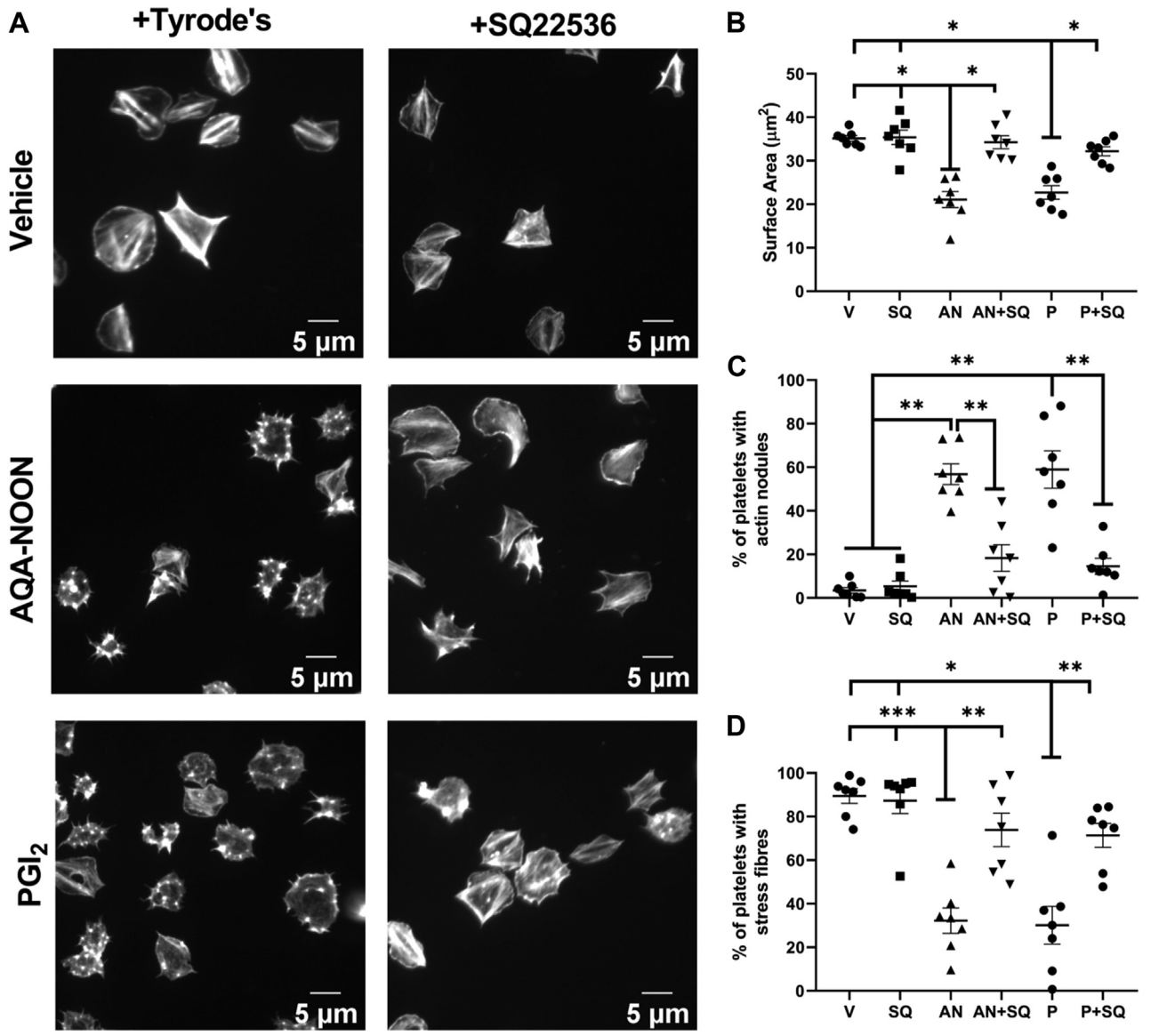

FIGURE 2 Zinc chelation–induced reversal of platelet spreading is blocked with the addition of the adenylyl cyclase inhibitor SQ22536. Platelets (2×10^7/mL) were treated with Tyrode (vehicle) or SQ22536 (100 µM) for 20 minutes, followed by spreading on 100 µg/mL fibrinogen for 25 minutes. They were then washed with phosphate-buffered saline and treated with Tyrode (vehicle), 2-((2-(2-(2-aminoethoxy) ethoxy)ethyl)amino)-N-(quinolin-8-yl)acetamide (AQA-NOON; 1 mM), or prostaglandin I_2 (10 nM). (A) Representative images. Scale bar is 5 µm. (B) Average surface area of spread platelets. (C) Percentage of platelets with actin nodules. (D) Percentage of platelets with stress fibers. Data are presented as mean ± SEM of n = 7. $^*p < .05$ and $^{**}p < .01$. AN, AQA-NOON; P, prostaglandin I_2; SQ, SQ22536; V, vehicle.

of Zn^{2+} in platelets, we assessed the effects of the Zn^{2+}-chelating agents TPEN, AQA-F, and a novel derivative of AQA-F, AQA-NOON on platelet function. All these agents have higher affinities for Zn^{2+} than for Ca^{2+} (Supplementary Figure S2A–D) [30,31]. While TPEN has been used previously in platelet studies, neither AQA-F nor AQA-NOON has been tested in platelets. However, AQA-F has been demonstrated to chelate Zn^{2+} in cancer cells, suggesting that AQA derivatives have the ability to cross the cell membrane [30]. Therefore, we assessed platelet aggregation stimulated with Zn^{2+}, thrombin, or collagen in the absence and presence of AQA-F, AQA-NOON, and TPEN each. All 3 chelating agents inhibited Zn^{2+}-induced platelet aggregation as expected (Supplementary Figures S2E–F). TPEN, AQA-F, and AQA-NOON also inhibited thrombin- and collagen-induced platelet aggregation in washed platelets and PRP in a dose-dependent manner (Supplementary Figures S3 and S4). Aggregation was significantly inhibited by 1 mM AQA-NOON and 100 µM AQA-F, while TPEN showed a significant effect at 30 µM. When the chelators were incubated for 20 minutes as opposed to 2 minutes prior to thrombin stimulation, there appeared to be an increase in inhibition of aggregation (Supplementary Figure S3). Due to this observation, we chose 20-minute treatment with the chelators as a starting time point for further experiments in the study. In addition and in agreement with a study by Ahmed et al. [15], treatment with either TPEN or AQA-NOON for 20 minutes prior to spreading on fibrinogen

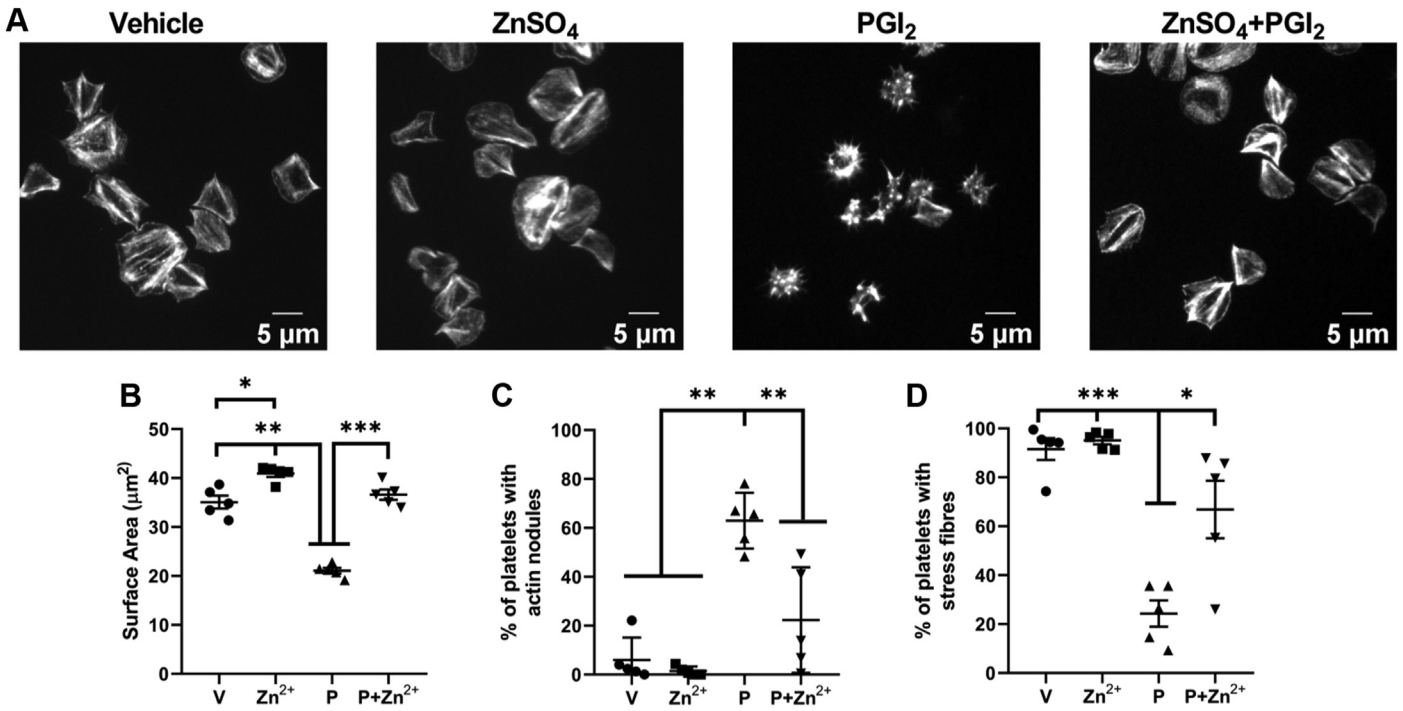

FIGURE 3 Addition of zinc significantly inhibits prostaglandin I_2–induced reversal of platelet spreading. Platelets (2×10^7/mL) were treated with Tyrode (vehicle) or zinc sulfate (100 µM) immediately prior to spreading on fibrinogen (100 µg/mL) for 25 minutes. They were then washed with phosphate-buffered saline and treated with either Tyrode (vehicle) or prostaglandin I_2 (PGI_2; 10 nM) for 20 minutes. (A) Representative images. Scale bar is 5 µm. (B) Surface area of spread platelets. (C) Percentage of platelets with actin nodules. (D) Percentage of platelets with stress fibers. Data are presented as mean ± SEM of n = 5. $^*p < .05$, $^{**}p < .01$, and $^{***}p < .001$. F, fibrinogen; P, prostaglandin I_2; V, vehicle; Zn^{2+}, zinc sulfate.

significantly reduced platelet surface area and platelet stress fiber formation (Supplementary Figure S5).

Although it is important that Zn^{2+} causes platelet activation, it is also important to understand if Zn^{2+} is required to maintain and sustain platelet activation. To assess this, we allowed platelets to spread on fibrinogen for 25 minutes before the addition of Zn^{2+} chelators for 20 minutes. Analysis of these data showed that there was no effect on platelet adhesion (Supplementary Figure S6A). However, there was a significant reduction of 13.99 ± 0.80 and 7.09 ± 1.44 μm^2 in surface area in the presence of AQA-NOON (1 mM) and TPEN (30 μM) respectively, in comparison with those in their respective controls (Figure 1A, B). Furthermore, analysis of the platelet actin structures showed a significant increase in actin nodule formation in response to both Zn^{2+} chelators (Figure 1A, C). Treatment with AQA-NOON also led to a significant reduction in the percentage of platelets with stress fibers (Figure 1A, D). The reduction in platelets with stress fibers and platelet surface area in the presence of Zn^{2+} chelators was like that identified with PGI_2 (10 nM) treatment [29]. In addition, posttreatment with BAPTA-AM had little effect on platelet adhesion or surface area, indicating that TPEN, AQA-F, and AQA-NOON were not mediating their effect through affecting calcium signaling (Supplementary Figure S7).

To further investigate the requirement for Zn^{2+} in maintaining platelet activity, we investigated if Zn^{2+} chelation would reverse thrombus formation. Therefore, we allowed thrombi to form on collagen before postperfusion with AQA-F, AQA-NOON, or TPEN. This demonstrated that postperfusion of these chelators caused significant reductions in thrombus surface area coverage and thrombus height (Figure 1E–G).

In summary, these data establish that Zn^{2+} is not only capable of causing platelet activation but also required to sustain activation, thereby maintaining thrombus formation and stability under high shear.

3.2 | Zn^{2+} regulates the PGI_2/cAMP/PKA pathway to maintain platelet activation

As we had demonstrated that Zn^{2+} chelation could both prevent and reverse platelet activation, we then investigated the mechanism by which this occurred. Consequently, we asked if the inhibitory effect of Zn^{2+} chelation was due to increased PGI_2 signaling. Therefore, we added the AC inhibitor SQ22536 (100 μM) to platelets prior to spreading on fibrinogen, followed by postspreading treatment with Zn^{2+} chelators. Interestingly, the reversal of platelet surface area and actin nodule formation induced by AQA-NOON, TPEN, or PGI_2 was significantly blocked by the addition of SQ22536, showing that this reversal was dependent on cAMP production. No effect on platelet adhesion was identified after any of the treatments or combination of treatments (Figure 2; Supplementary Figures S8 and S9).

Next, we performed spreading experiments to show that addition of Zn^{2+} could prevent the action of PGI_2 signaling on platelets. Here, platelets were spread in the presence or absence of Zn^{2+} (100 μM) for 25 minutes before the addition of PGI_2 (10 nM) for 20 minutes. Analysis of these data showed that there was no effect on platelet adhesion (Supplementary Figure S10). Importantly, the addition of PGI_2 did not cause reversal in the presence of additional Zn^{2+}, whereas platelets that spread in the absence of Zn^{2+} and stimulated with PGI_2 significantly reduced their surface area and showed modulation of their actin structures, with a significant reduction in stress fibers and increase in actin nodules (Figure 3A–D). To confirm this effect in suspension, we performed aggregations to demonstrate that Zn^{2+} could prevent PGI_2-induced inhibition of platelet aggregation stimulated by thrombin. Here, we incubated platelets with Zn^{2+} (50 μM) for 13 minutes prior to the addition of PGI_2 (1 nM) for 2 minutes, followed by stimulation with thrombin (0.01 U/mL), and monitored aggregation. The data demonstrated that as expected, Zn^{2+} addition could significantly potentiate thrombin-induced platelet aggregation, whereas PGI_2 significantly inhibited platelet aggregation. However, in the presence of Zn^{2+}, PGI_2 had little effect, with aggregation being the same as thrombin alone (Supplementary Figure S11A, B).

These data, combined with SQ22536 inhibiting the effect of Zn^{2+} chelation on reversing platelet activation, suggest that Zn^{2+} can regulate platelet PGI_2 signaling.

3.3 | Zn^{2+} chelation elevates PGI_2 signaling in platelets

Although we had shown that Zn^{2+} could modulate PGI_2 signaling in activated platelets, we wished to see how basal platelets responded to the removal of Zn^{2+}. Therefore, we incubated basal washed platelets in the presence and absence of AQA-F (100 μM), AQA-NOON (1 mM), and TPEN (30 μM) for up to 40 minutes before lysis to analyze platelet $pVASP^{ser157}$ and total pPKA signaling. Platelets stimulated with PGI_2 (5 nM) were used as a positive control. Analysis of these data indicated that platelets, in the presence of AQA-F, AQA-NOON, and TPEN, induced significant elevation of $pVASP^{ser157}$ levels at 20, 30, and 40 minutes and total pPKA at 40 minutes (Figure 4A–C; Supplementary Figure S12). In contrast, PGI_2 induces a stronger $pVASP^{ser157}$ response, but this response is reduced over time, and by 20 minutes after stimulation, has significantly reduced (Figure 4D).

Overall, these data together demonstrate that Zn^{2+} can inhibit PGI_2 signaling, while Zn^{2+} chelation elevates PGI_2 signaling, leading to elevated and sustained levels of platelet inhibition.

3.4 | Zn^{2+} controls PGI_2 signaling through modulation of AC

Although it is clear that Zn^{2+} can modify PGI_2 signaling, it is necessary to understand how this occurs. There are 2 key enzymes in PGI_2 signaling whose modulation has been shown previously to affect platelet inhibition, AC, and PDE [26,32]. Therefore, to understand the mechanism, we initially spread platelets on fibrinogen in the presence and absence of Zn^{2+}. The platelets were then treated with either

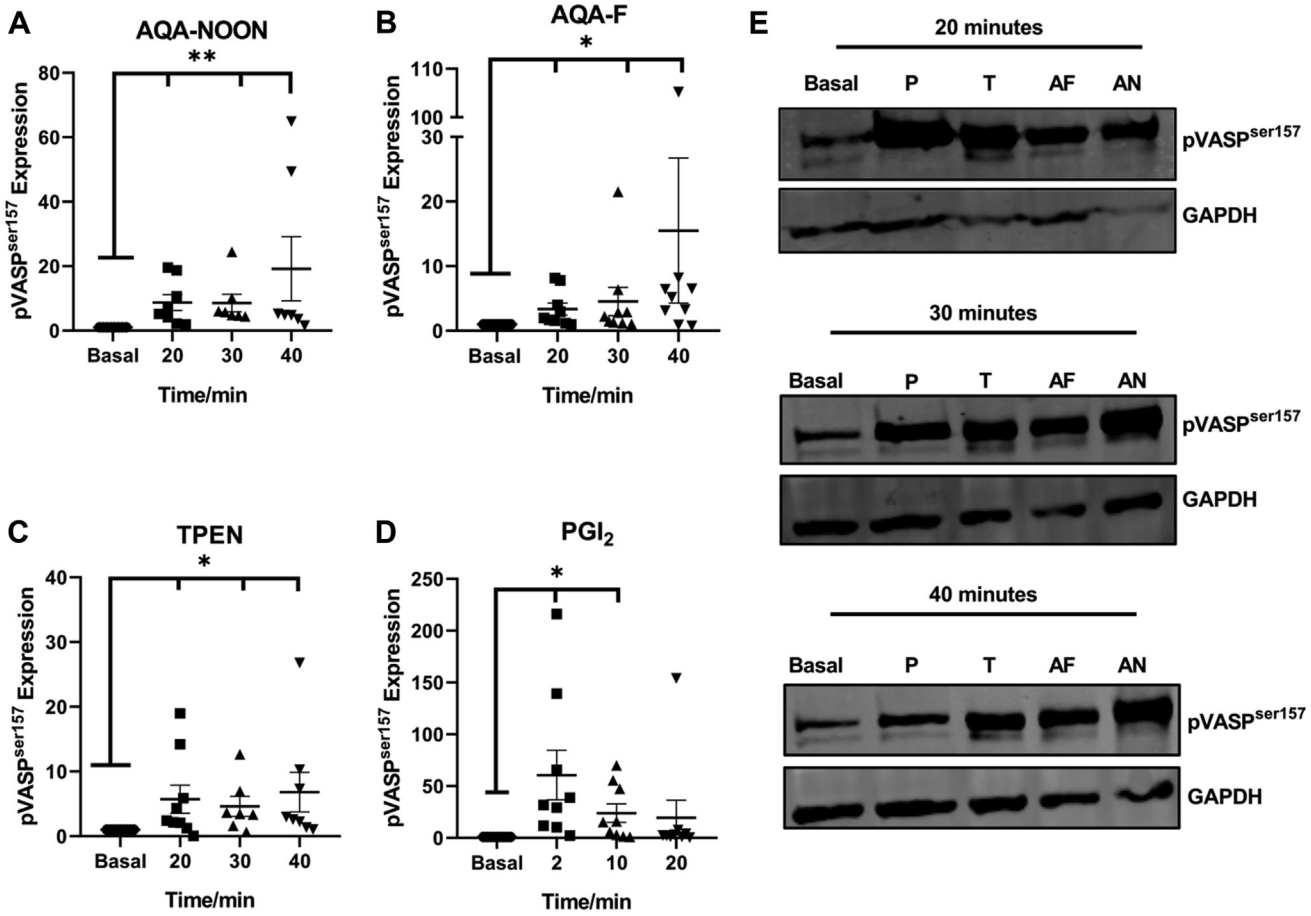

FIGURE 4 Zinc chelation significantly elevates resting $VASP^{ser157}$ phosphorylation. Washed platelets (4×10^8/mL) were incubated with 2-((2-(2-(2-aminoethoxy)ethoxy)ethyl)amino)-N-(quinolin-8-yl)acetamide (AQA-NOON; 1 mM), *N,N,N',N'*-tetrakis(2-pyridylmethyl) ethylenediamine (TPEN; 30 μM), or 2-((2-(2-fluoroethoxy)ethyl)amino)-N-(quinolin-8-yl)acetamide (AQA-F; 100 μM), and samples were taken at 20, 30, and 40 minutes and lysed with Laemmli buffer. Prostaglandin I_2 (PGI_2; 5 nM) was incubated with washed platelets, and samples were taken at 2, 10, and 20 minutes and lysed with Laemmli buffer. Phosphorylation of $VASP^{ser157}$ and GAPDH was then analyzed using immunoblotting. (A–D) Densitometric analysis of $pVASP^{ser157}$ bands after treatment with AQA-NOON (n = 8), AQA-F (n = 9), TPEN (n = 9), and/or PGI_2 (n = 7). E. Representative Western blots for $pVASP^{ser157}$ 20, 30, and 40 minutes after chelator treatment. Data are presented as mean ± SEM. $^*p < .05$ and $^{**}p < .01$. AF, AQA-F; AN, AQA-NOON; P, prostaglandin I_2; PGI_2, prostaglandin I_2; T, *N,N,N',N'*-tetrakis (2-pyridylmethyl)ethylenediamine; TPEN, *N,N,N',N'*-tetrakis(2-pyridylmethyl)ethylenediamine.

forskolin (10 μM) to activate AC or milrinone (10 μM) to inhibit phosphodiesterase 3 (PDE3). Analysis of these data showed that there was no effect on platelet adhesion (Supplementary Figure S13). While in the absence of Zn^{2+}, treatment with milrinone caused significant reversal of platelet spreading and stress fiber formation as expected, in the presence of Zn^{2+}, milrinone no longer reversed platelet activation (Figure 5). This indicated that AC was not functional. Interestingly, even the presence of the AC activator forskolin in the presence of Zn^{2+} had little effect on platelet activation, while in absence of Zn^{2+}, it caused reduction in platelet surface area and reversal of platelet stress fibers. Therefore, these data suggest that addition of Zn^{2+} blocks the constitutive activity of AC rather than increasing PDE3 activity to abrogate cAMP signaling.

To further confirm that Zn^{2+} modulates AC activity and does not target PGI_2 signaling, we investigated whether Zn^{2+} could regulate the inhibitory effects of PGE_2, which are known to be driven by AC [33]. To do this, platelets were spread in the presence or absence of Zn^{2+} (100 μM) for 25 minutes before the addition of PGE_2 (100 nM) for 20 minutes. Analysis of these data showed that there was no effect on platelet adhesion. Importantly, the addition of PGE_2 did not cause reversal in the presence of additional Zn^{2+}, whereas platelets that spread in the absence of Zn^{2+} and stimulated with PGE_2 significantly reduced their surface area and showed modulation of their actin structures, with a significant reduction in stress fibers and increase in actin nodules (Supplementary Figure S14). In agreement, PGE_2 (100 nM) significantly inhibited aggregation to thrombin (0.01 U/mL), which was abrogated in the presence of Zn^{2+} (50 μM). Interestingly, we found that low-dose PGE_2 (10 nM) did not potentiate platelet aggregation, in contrast to previous studies (data not shown) [34].

Overall, these data show that Zn^{2+} likely acts to directly inhibit platelet AC rather than increase PDE3 activity.

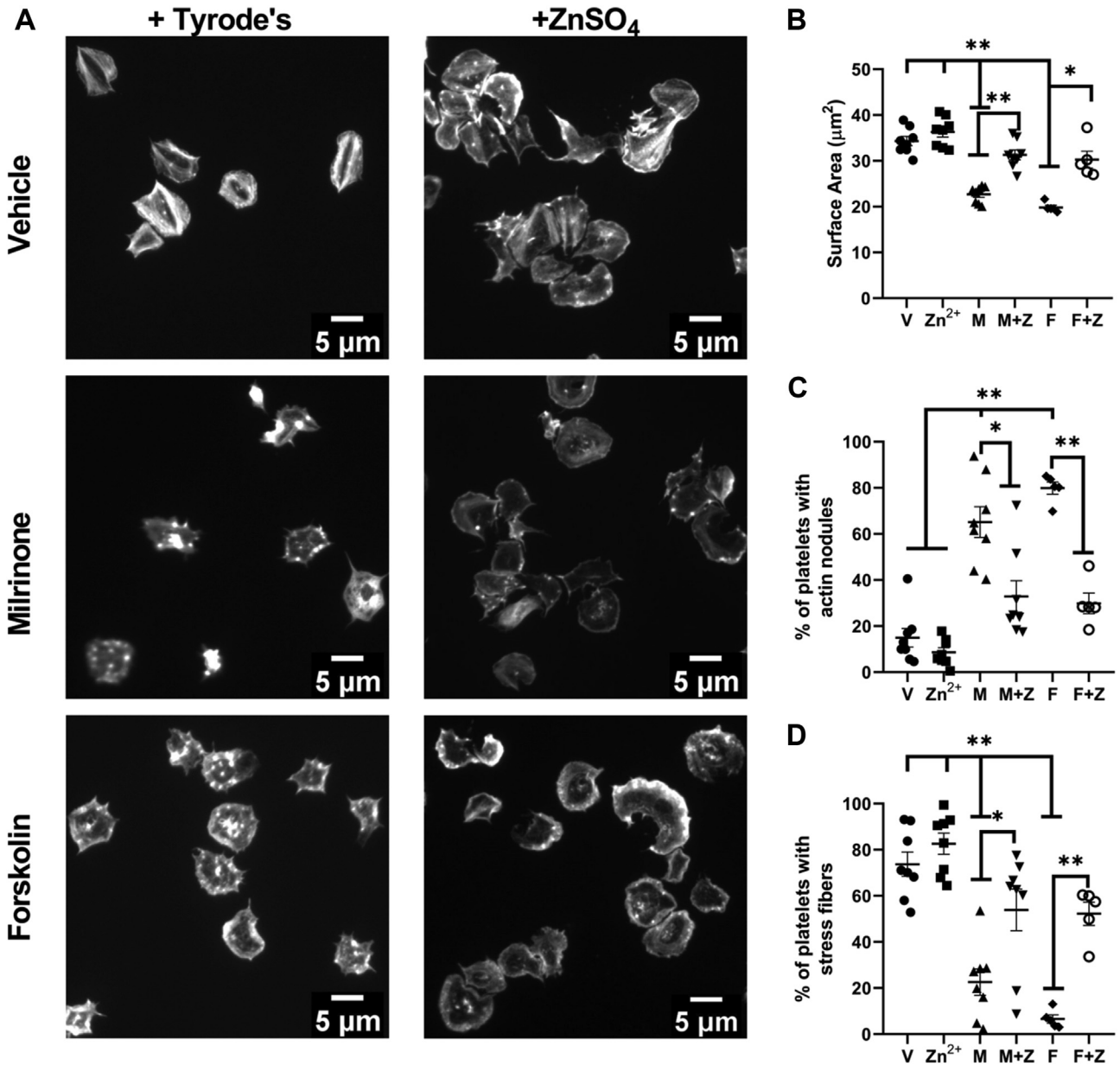

FIGURE 5 Addition of zinc significantly inhibits milrinone- and forskolin-induced reversal of platelet spreading. Platelets (2×10^7/mL) were treated with Tyrode (vehicle) or zinc sulfate (100 µM) immediately prior to spreading on 100 µg/mL fibrinogen for 25 minutes. They were then washed with phosphate-buffered saline and treated with either Tyrode (vehicle), milrinone (10 µM), or forskolin (10 µM) for 20 minutes. (A) Representative images. Scale bar is 5 µm. (B) Surface area of spread platelets. (C) Percentage of platelets with actin nodules. (D) Percentage of platelets with stress fibers. Data are presented as mean ± SEM of n = 5 (forskolin) and n = 8 (milrinone). *$p < .05$ and **$p < .01$. F, forskolin; M, milrinone; V, vehicle; Z, zinc sulfate; Zn^{2+}, zinc sulfate; $ZnSO_4$, zinc sulfate.

3.5 | Zn^{2+} chelation potentiates PGI_2 signaling in both washed platelets and whole blood

As we had shown that Zn^{2+} can inhibit PGI_2 signaling via regulation of AC, while the Zn^{2+} chelators AQA-F, AQA-NOON, and TPEN could all induce elevation of $pVASP^{ser157}$ and total pPKA substrate levels, we next investigated if this would mean that Zn^{2+} chelation would potentiate PGI_2 signaling in platelets. Therefore, we incubated platelets with AQA-F (10 µM), AQA-NOON (1 mM), or TPEN (3 µM) for 18 minutes before the addition of PGI_2 (5 nM) for 2 minutes, followed by stimulation with thrombin (0.1 U/mL), and monitored platelet aggregation. The data clearly showed that PGI_2 or Zn^{2+} chelators separately did not significantly affect platelet aggregation. However, in combination, they inhibited platelet aggregation fully (Figure 6A–B; Supplementary Figure S15).

To confirm our results in whole blood, we performed *in vitro* flow to monitor thrombus formation in the presence and absence of both Zn^{2+} chelators and PGI_2. The doses of Zn^{2+} chelators or PGI_2 (300 pM) had little effect by themselves. However, incubation with AQA-NOON (0.3 mM), AQA-F (10 µM), or TPEN (3 µM) for 18 minutes followed by PGI_2 (300 pM) treatment for 2 minutes strongly inhibited thrombus surface area coverage, demonstrating the potentiation of

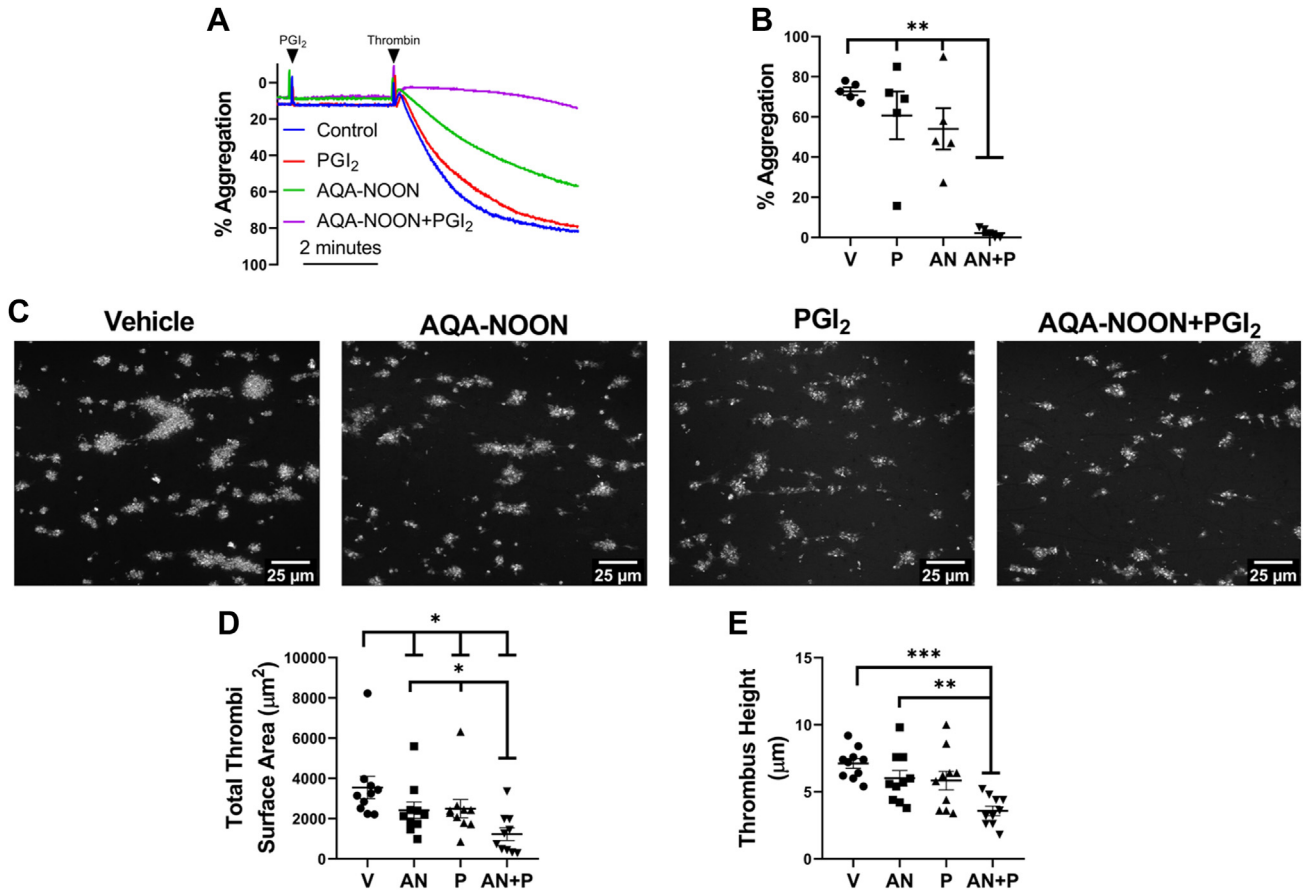

FIGURE 6 Zinc chelation synergizes with prostaglandin I_2 (PGI_2) to significantly inhibit platelet aggregation and thrombus formation. For aggregations, washed platelets (2.5×10^8/mL) were treated with either 2-((2-(2-(2-aminoethoxy)ethoxy)ethyl)amino)-N-(quinolin-8-yl) acetamide (AQA-NOON; 1 mM, n = 5) Tyrode (vehicle) for 18 minutes, followed by treatment with PGI_2 (5 nM) or Tyrode for 2 minutes. The platelets were then stimulated with thrombin (0.1 U/mL). For *in vitro* thrombus formation, whole blood was treated with AQA-NOON (300 µM) or Tyrode (vehicle) for 18 minutes, followed by treatment with PGI_2 (300 pM) for 2 minutes. Whole blood was then flowed over collagen (25 µg/mL)-coated biochips for 2 minutes. (A) Representative traces of the aggregations. (B) Percentage aggregation at 5 minutes after stimulation with thrombin (0.1 U/mL) following treatment with AQA-NOON or AQA-NOON + PGI_2. (C) Representative images. Scale bar is 20 µm. (D) Analysis of the total surface area of the image covered by thrombi. (E) Analysis of thrombus height. Data are presented as mean ± SEM. For *in vitro* thrombus formation, n = 10 for AQA-NOON. Data are presented as mean ± SEM. $^*p < .05$, $^{**}p < .01$, and $^{***}p < .001$. AN, AQA-NOON; P, prostaglandin I_2; PGI_2, prostaglandin I_2; V, vehicle.

inhibitory signaling on thrombus formation (Figure 6C–E; Supplementary Figure S16). This clearly indicated that Zn^{2+} chelation, therefore, induced potentiation of the effect of PGI_2.

4 | DISCUSSION

Although easily treatable with supplementation and not common in the Western world, Zn^{2+} deficiency is still highly prevalent worldwide [1]. Consequently, the bleeding diathesis that results from Zn^{2+} deficiency is still relevant, including in clinically relevant populations in the Western world, such as patients with cancer [35]. Thus, it is still important that the mechanisms behind this diathesis are elucidated.

Here, we present the first evidence that Zn^{2+} can act as a powerful regulator of platelet inhibitory signaling. Our data demonstrated that Zn^{2+} is essential for thrombus stability and the maintenance of platelet activation; Zn^{2+} chelation can reverse platelet activity via modulation of AC and, in suspension, can lead to a sustained increase in platelet $VASP^{ser157}$ and PKA substrate phosphorylation; fluctuations in platelet Zn^{2+} can modulate platelet PGI_2 signaling by inhibiting the activity of AC; and functionally, Zn^{2+} chelation can synergize with PGI_2 to inhibit platelet activity and thrombus formation *in vitro*. Our data, therefore, build on the proposed role of Zn^{2+} as a second messenger to potentiate platelet activation [10,15].

Here our work agrees with past studies that showed that Zn^{2+} is essential for platelet function, demonstrating that Zn^{2+} removal prior to platelet stimulation results in impaired platelet activation [13,15,16,36]. It must be noted, however, that there needs to be a relevant timeframe to induce full Zn^{2+} chelation. Although all the chelators used had the ability to cross the cell membrane, they required up to 20 minutes to induce their full effect. Importantly, here, we also demonstrated that Zn^{2+} is required to maintain platelet activation as when it is removed after activation, platelets reduce their level of activity. As a consequence of this, thrombus formation is

reversed when Zn^{2+} is chelated. Therefore, physiologically, Zn^{2+} is required not only to help but also maintain platelet activation. One caveat is that we cannot be sure that all Zn^{2+} has been chelated within the platelet as the level of Zn^{2+} is dependent on the individual. This may, in part, help explain why some donors were highly responsive while others were less responsive to the presence of Zn^{2+} chelators. As part of this, the effect of Zn^{2+} chelation on integrin activation is unclear. The data suggest that platelet adhesion was unaffected in the presence of the Zn^{2+} chelators, but potentially, Zn^{2+}, which was not chelated, may have been high enough to reduce the effects on integrin activation. Therefore, the role of Zn^{2+} in platelet integrin function is an area for future research.

Due to the significant inhibitory effect of Zn^{2+} chelation, we asked if Zn^{2+} could modulate PGI_2-cAMP-PKA signaling. Platelet PGI_2 signaling is essential for preventing aberrant platelet activation [21]. PGI_2 activates AC, elevating cAMP concentration, which in turn activates PKA and causes "global" inhibition of platelet activation [37,38]. Interestingly, previous data have shown that Zn^{2+} could directly alter AC activity in other cell types [20,27]. Our data demonstrated that Zn^{2+} chelation increases basal platelet $pVASP^{ser157}$ and total pPKA phosphorylation, indicating a possible increase in platelet AC activity or cAMP production. This is important as AC is constitutively active in platelets, and Zn^{2+} is, therefore, potentially critical in controlling its activity and the basal level of inhibition experienced by platelets.

To elucidate the mechanism via which Zn^{2+} regulates the PGI_2 pathway, we spread platelets with Zn^{2+} and attempted to reverse platelet activation with the direct AC agonist forskolin and the PDE3a inhibitor milrinone. Interestingly, Zn^{2+} inhibited the effect of both forskolin and milrinone, suggesting that Zn^{2+} directly regulates AC and is not required for driving PDE3a activity. In agreement, we investigated the effect of PGE_2, which has been shown to target prostaglandin E receptor 3 (EP3) receptors, which are linked to AC [33]. Zn^{2+} also prevented the inhibition of platelet activation by PGE_2, indicating that both PGE_2 and PGI_2, which work in similar manners to inhibit platelet, are affected by the level of Zn^{2+}. Therefore, we demonstrated the first evidence that AC is directly regulated by Zn^{2+} in platelets.

Moreover, we also showed that Zn^{2+} chelation affected PGI_2 signaling by elevating its effectiveness. Our aggregation and flow data both showed clearly that Zn^{2+} chelation dramatically increased the ability of PGI_2 to inhibit platelet function. Critically, in our flow experiments, we used 300pM PGI_2, a dose thought to be close to the physiologic level of PGI_2 to prevent thrombus formation in the presence of Zn^{2+} chelators [39]. This suggests that physiologically, even a small decrease in platelet and/or plasma Zn^{2+} can lead to potentiation of PGI_2 signaling with the potential to cause subsequent disruption of hemostasis, leading to a bleeding phenotype.

Importantly, it was recently demonstrated by Sobczak et al. [40] that nonesterified fatty acids present in patients with type 2 diabetes can displace Zn^{2+} from its primary plasma transporter human serum albumin. This displacement led to increased plasma Zn^{2+}, resulting in increased platelet aggregation, fibrin clot density, and fibrin fiber thickness. In addition, it was demonstrated by Kahal et al. [41] that patients with type 2 diabetes have decreased PGI_2 sensitivity after 24 hours of hypoglycemia. This change in PGI_2 sensitivity, alongside the elevation in Zn^{2+} levels, could be explained by our data. Our data would provide a novel mechanism explaining the reduced PGI_2 sensitivity in patients with type 2 diabetes after hypoglycemia and a possible mechanism contributing to the prothrombotic nature of type 2 diabetes platelets. Although our study used Zn^{2+} at 50 to 100 μM to regulate platelet cAMP signaling, future work could focus on the effects of small increases in Zn^{2+} at more physiologic levels. For example, the effect on platelet PGI_2 activity if plasma Zn^{2+} is raised by a small amount from its physiologic 10 to 20 μM [17].

In conclusion, our data present the first evidence that Zn^{2+} can modulate platelet activity by regulation of AC and subsequently altered platelet prostaglandin signaling. Our data suggest that when Zn^{2+} is secreted from granules during platelet activation, labile Zn^{2+} re-entering the platelets could increase platelet activity by inhibiting AC activity and downregulating PGI_2 signaling. This then potentiates responses from platelet agonists, drives fibrin formation, and ultimately proliferates thrombus formation. This could partially explain the data of Watson et al. [13] that low levels of Zn^{2+} can potentiate responses to thrombin, collagen, and adrenaline. However, in a state of Zn^{2+} deficiency, be it chelator induced or dietarily induced, Zn^{2+} is not present in high enough concentrations to prevent AC activity, and therefore, PGI_2 signaling is abnormally increased, leading to reduced platelet activity. This ability to regulate PGI_2 signaling results in Zn^{2+} being essential for both initiation and maintenance of platelet activation, suggesting that Zn^{2+} chelation could be used as a potential future antiplatelet therapy.

Overall, in a clinical context, our data demonstrate that Zn^{2+} chelation or deficiency could cause an elevation in PGI_2 signaling, leading to increased platelet inhibition and the inability to effectively form a thrombus. Conversely, small increases in plasma Zn^{2+} in diseases such as type 2 diabetes could dysregulate PGI_2 activity, leading to prothrombotic platelets contributing to the atherothrombosis associated with these diseases.

ACKNOWLEDGMENTS

The authors would like to thank Tim Palmer for technical advice and editorial assistance.

AUTHOR CONTRIBUTIONS

S.D.J.C. and G.J.S. designed and supervised the study. C.A.C., L.N.-A., and Z.B. conducted the main experiments. Y.A. conducted the experiments for the study. T.W.P., G.F., and M.A. provided novel chelators for the experiments. C.A.C. conducted all data analysis. C.A.C. and S.D.J.C. drafted the manuscript. All authors edited the manuscript as well as read and approved the final version of the paper.

DECLARATION OF COMPETING INTERESTS

There are no competing interests to disclose.

REFERENCES

[1] Wessells KR, Brown KH. Estimating the global prevalence of zinc deficiency: results based on zinc availability in national food supplies and the prevalence of stunting. *PLoS One*. 2012;7:e50568.

[2] Andreini C, Bertini I. A bioinformatics view of zinc enzymes. *J Inorg Biochem*. 2012;111:150–6.

[3] Prasad AS, Halsted JA, Nadimi M. Syndrome of iron deficiency anemia, hepatosplenomegaly, hypogonadism, dwarfism and geophagia. *Am J Med*. 1961;31:532–46.

[4] Lin PH, Sermersheim M, Li H, Lee PHU, Steinberg SM, Ma J. Zinc in wound healing modulation. *Nutrients*. 2017;10:16.

[5] Keen CL, Gershwin ME. Zinc deficiency and immune function. *Annu Rev Nutr*. 1990;10:415–31.

[6] Gordon PR, Woodruff CW, Anderson HL, O'Dell BL. Effect of acute zinc deprivation on plasma zinc and platelet aggregation in adult males. *Am J Clin Nutr*. 1982;35:113–9.

[7] Cohen JA, Leeksma CH. Determination of the life span of human blood platelets using labelled diisopropylfluorophosphonate. *J Clin Invest*. 1956;35:964–9.

[8] Mason KD, Carpinelli MR, Fletcher JI, Collinge JE, Hilton AA, Ellis S, Kelly PN, Ekert PG, Metcalf D, Roberts AW, Huang DCS, Kile BT. Programmed anuclear cell death delimits platelet life span. *Cell*. 2007;128:1173–86.

[9] Noris P, Biino G, Pecci A, Civaschi E, Savoia A, Seri M, Melazzini F, Loffredo G, Russo G, Bozzi V, Notarangelo LD, Gresele P, Heller PG, Pujol-Moix N, Kunishima S, Cattaneo M, Bussel J, De Candia E, Cagioni C, Ramenghi U, et al. Platelet diameters in inherited thrombocytopenias: analysis of 376 patients with all known disorders. *Blood*. 2014;124:e4–10.

[10] Kiran Gotru S, van Geffen JP, Nagy M, Mammadova-Bach E, Eilenberger J, Volz J, Manukjan G, Schulze H, Wagner L, Eber S, Schambeck C, Deppermann C, Brouns S, Nurden P, Greinacher A, Sachs U, Nieswandt B, Hermanns HM, Heemskerk JWM, Braun A. Defective Zn^{2+} homeostasis in mouse and human platelets with alpha- and delta-storage pool diseases. *Sci Rep*. 2019;9:8333.

[11] Meyers KM, Holmsen H, Seachord CL. Comparative study of platelet dense granule constituents. *Am J Physiol*. 1982;243:R454–61.

[12] Jonnalagadda D, Izu LT, Whiteheart SW. Platelet secretion is kinetically heterogeneous in an agonist-responsive manner. *Blood*. 2012;120:5209–16.

[13] Watson BR, White NA, Taylor KA, Howes JM, Malcor JD, Bihan D, Sage SO, Farndale RW, Pugh N. Zinc is a transmembrane agonist that induces platelet activation in a tyrosine phosphorylation-dependent manner. *Metallomics*. 2016;8:91–100.

[14] Lopes-Pires ME, Ahmed NS, Vara D, Gibbins JM, Pula G, Pugh N. Zinc regulates reactive oxygen species generation in platelets. *Platelets*. 2021;32:368–77.

[15] Ahmed NS, Lopes Pires ME, Taylor KA, Pugh N. Agonist-evoked increases in intra-platelet zinc couple to functional responses. *Thromb Haemost*. 2019;119:128–39.

[16] Emery MP, O'Dell BL. Low zinc status in rats impairs calcium uptake and aggregation of platelets stimulated by fluoride. *Proc Soc Exp Biol Med*. 1993;203:480–4.

[17] Foote JW, Delves HT. Albumin bound and alpha 2-macroglobulin bound zinc concentrations in the sera of healthy adults. *J Clin Pathol*. 1984;37:1050–4.

[18] Marx G, Krugliak J, Shaklai M. Nutritional zinc increases platelet reactivity. *Am J Hematol*. 1991;38:161–5.

[19] Klein C, Heyduk T, Sunahara RK. Zinc inhibition of adenylyl cyclase correlates with conformational changes in the enzyme. *Cell Signal*. 2004;16:1177–85.

[20] Klein C, Sunahara RK, Hudson TY, Heyduk T, Howlett AC. Zinc inhibition of cAMP signaling. *J Biol Chem*. 2002;277:11859–65.

[21] Smolenski A. Novel roles of cAMP/cGMP-dependent signaling in platelets. *J Thromb Haemost*. 2012;10:167–76.

[22] Beck F, Geiger J, Gambaryan S, Veit J, Vaudel M, Nollau P, Kohlbacher O, Martens L, Walter U, Sickmann A, Zahedi RP. Time-resolved characterization of cAMP/PKA-dependent signaling reveals that platelet inhibition is a concerted process involving multiple signaling pathways. *Blood*. 2014;123:e1–10.

[23] Harbeck B, Hüttelmaier S, Schlüter K, Jockusch BM, Illenberger S. Phosphorylation of the vasodilator-stimulated phosphoprotein regulates its interaction with actin. *J Biol Chem*. 2000;275:30817–25.

[24] Horstrup K, Jablonka B, Hönig-Liedl P, Just M, Kochsiek K, Walter U. Phosphorylation of focal adhesion vasodilator-stimulated phosphoprotein at Ser157 in intact human platelets correlates with fibrinogen receptor inhibition. *Eur J Biochem*. 1994;225:21–7.

[25] Mellwig KP, Jakobs KH. Inhibition of platelet adenylate cyclase by ADP. *Thromb Res*. 1980;18:7–17.

[26] Zhang W, Colman RW. Thrombin regulates intracellular cyclic AMP concentration in human platelets through phosphorylation/activation of phosphodiesterase 3A. *Blood*. 2007;110:1475–82.

[27] Katsel PL, Tagliente TM, Schwarz TE, Craddock-Royal BD, Patel ND, Maayani S. Molecular and biochemical evidence for the presence of type III adenylyl cyclase in human platelets. *Platelets*. 2003;14:21–33.

[28] Aburima A, Wraith KS, Raslan Z, Law R, Magwenzi S, Naseem KM. cAMP signaling regulates platelet myosin light chain (MLC) phosphorylation and shape change through targeting the RhoA-Rho kinase-MLC phosphatase signaling pathway. *Blood*. 2013;122:3533–45.

[29] Yusuf MZ, Raslan Z, Atkinson L, Aburima A, Thomas SG, Naseem KM, Calaminus SDJ. Prostacyclin reverses platelet stress fibre formation causing platelet aggregate instability. *Sci Rep*. 2017;7:5582.

[30] Price TW, Firth G, Eling CJ, Kinnon M, Long NJ, Sturge J, Stasiuk GJ. A 18F radiolabelled Zn(II) sensing fluorescent probe. *Chem Commun*. 2018;54:3227–30.

[31] Shumaker DK, Vann LR, Goldberg MW, Allen TD, Wilson KL. TPEN, a Zn^{2+}/Fe^{2+} chelator with low affinity for Ca^{2+}, inhibits lamin assembly, destabilizes nuclear architecture and may independently protect nuclei from apoptosis in vitro. *Cell Calcium*. 1998;23:151–64.

[32] Zieve PD, Greenough WB III. Adenyl cyclase in human platelets: activity and responsiveness. *Biochem Biophys Res Commun*. 1969;35:462–6.

[33] Smith JP, Haddad EV, Downey JD, Breyer RM, Boutaud O. PGE2 decreases reactivity of human platelets by activating EP2 and EP4. *Thromb Res*. 2010;126:e23–9.

[34] Vezza R, Roberti R, Nenci GG, Gresele P. Prostaglandin E2 potentiates platelet aggregation by priming protein kinase C. *Blood*. 1993;82:2704–13.

[35] Stefanini M. Cutaneous bleeding related to zinc deficiency in two cases of advanced cancer. *Cancer*. 1999;86:866–70.

[36] Faure P, Durand P, Blache D, Favier A, Roussel AM. Influence of a long-term zinc-deficient diet on rat platelet function and fatty acid composition. *Biometals*. 1995;8:80–5.

[37] Moncada S, Gryglewski R, Bunting S, Vane JR. An enzyme isolated from arteries transforms prostaglandin endoperoxides to an unstable substance that inhibits platelet aggregation. *Nature*. 1976;263:663–5.

[38] Gorman RR, Bunting S, Miller OV. Modulation of human platelet adenylate cyclase by prostacyclin (PGX). *Prostaglandins*. 1977;13:377–88.

[39] Borgdorff P, Tangelder GJ, Paulus WJ. Cyclooxygenase-2 inhibitors enhance shear stress-induced platelet aggregation. *J Am Coll Cardiol*. 2006;48:817–23.

[40] Sobczak AIS, Katundu KGH, Phoenix FA, Khazaipoul S, Yu R, Lampiao F, Stefanowicz F, Blindauer CA, Pitt SJ, Smith TK, Ajjan RA, Stewart AJ. Albumin-mediated alteration of plasma zinc speciation by fatty acids modulates blood clotting in type-2 diabetes. *Chem Sci*. 2021;12:4079–93.

[41] Kahal H, Aburima A, Spurgeon B, Wraith KS, Rigby AS, Sathyapalan T, Kilpatrick ES, Naseem KM, Atkin SL. Platelet function following induced hypoglycaemia in type 2 diabetes. *Diabetes Metab*. 2018;44:431–6.

SUPPLEMENTARY MATERIAL

The online version contains supplementary material available at https://doi.org/10.1016/j.jtha.2023.05.008